Journal
Artificial Cells, Nanomedicine, and Biotechnology >
An International Journal
Volume 46, 2018 - Issue 1

Original Articles

Nefopam hydrochloride loaded microspheres for post-operative pain management: synthesis, physicochemical characterization and *in-vivo* evaluation

Neelam Sharma, Sandeep Arora & Jitender Madan

Pages 138-146 | Received 22 Nov 2016, Accepted 27 Feb 2017, Published online: 21 Mar 2017

Download citation https://doi.org/10.1080/21691401.2017.1301459

Full Article Figures & data References Citations Metrics Reprints & Permissions

Abstract

Once-daily oral dosage of nefopam hydrochloride loaded sustained release microspheres (NPH-MS) was investigated as novel therapeutic strategy for post-operative pain management. Microspheres were synthesized using poly-3-hydroxybutyrate and poly-(ε-caprolactone) by double emulsion solvent evaporation technique. NPH-MS were characterized through FTIR, PXRD and SEM. *In-vitro* drug release study revealed sustained behavior till 24 h. Haemolysis was <5% which signified haemocompatibility of formulation. ED50 in rat tail-flick anti-nociceptive test was found ~18.12 mg/kg. In post-operative pain model, reversal of mechanical allodynia and thermal hyperalgesia by NPH-MS was statistically significant ($p < .001$) as compared with NPH till 24 h post-dose.

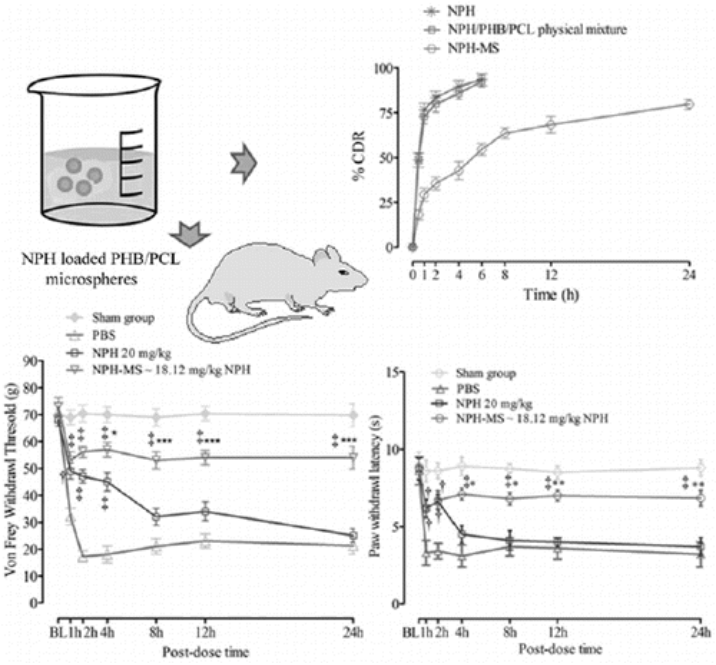

Keywords: Poly-3-hydroxybutyrate, poly-(ε-caprolactone), sustained release microspheres, haemocompatibility, anti-nociceptive, mechanical allodynia, thermal hyperalgesia, post-operative pain model

Introduction

The investigations in drug delivery involve sustained release of an active entity to curtail dosage frequency, diminution in toxicity though retaining therapeutic effectiveness of dosage regimen, improved bioavailability of active pharmaceutical moiety with superior safety and biocompatibility [1]. Nefopam hydrochloride (NPH) (Figure 1(a)) is non-opioid centrally acting analgesic preferred for relief of nociception in different pain syndrome such as acute traumatic, surgical operations, toothache and myalgia. Recommended oral dosage of NPH is 30–90 mg three times daily which might produce patient non-compliance and additional side effects such as dry mouth, hypersensitivity, patch necrosis of gastrointestinal mucosa, nausea and vomiting [2,3]. Therefore, development of biodegradable sustained release polymeric microspheres of NPH has been superlative methodology to reduce dosage frequency [4].

Figure 1. Chemical structure of (a) nefopam hydrochloride, (b) poly-3-hydroxybutyrate, and (c) poly-ε-caprolactone.

Display full size

Poly-3-hydroxybutyrate (PHB) (Figure 1(b)) and poly-ε-caprolactone (PCL) (Figure 1(c)) had been utilized as drug carriers owing to their biodegradability *via* hydrolytic cleavage of ester bonds into non-toxic end-products which can be eliminated from body *via* natural metabolic pathways [5–7]. Since, amorphous regions of semicrystalline PCL degrade prior to crystalline domains leading to change in drug release profile. Therefore, blend of PHB and PCL merge specific characteristic from individual polymer for controlling drug release pattern from microspheres [8–10].

In current investigation, novel sustained release nefopam hydrochloride loaded microspheres (NPH-MS) were manufactured for effective management of post-operative pain condition. Antinociceptive tail-flick activity of NPH-MS was executed to determine its effective oral dose (ED_{50}) in rat model. Magnitude of reversal of mechanical allodynia and thermal hyperalgesia produced by NPH-MS was compared with NPH using post-operative pain model. Behavioral signs of allodynia and hyperalgesia were von frey withdrawal threshold (VFWT) and paw withdrawal latency (PWL) in von Frey and plantar test, respectively.

Materials and methods

Materials

Poly ε-caprolactone (CAS No-24980-41-4, $(C_6H_{10}O_2)_n$, average M_w ~14,000, average M_n ~10,000 by GPC) and polyhydroxybutyrate (CAS No-29435-48-1, poly-(R)-3-hydroxybutyric acid) were purchased from Sigma–Aldrich Chemie, Gmbh, Steinhelm, Germany. Nefopam hydrochloride (M_w 289.8 g/mol, 99.57% purity) was purchased from Hangzhou-Daying-Chem. Company Ltd., China. All other chemicals used were of analytical grade.

Fabrication of NPH-loaded PHB/PCL biodegradable microspheres

NPH-MS were fabricated using double emulsion solvent evaporation technique (Figure 2) [11,12]. Briefly, aqueous solution of NPH (1 part) was prepared in distilled water:acetone (1:1) mixture. Polymer blend (3 part) containing PHB:PCL (1:1) was incorporated in dichloromethane (10 mL) to produce organic

phase. Aqueous solution was extruded slowly through syringe #20 to organic phase containing 0.5% w/v sorbitan monooleate as an emulsifier followed by sonication for 2 min at 55 W on an ice bath using an ultrasonic probe sonicator (PCI analyticals, India). Primary emulsion was added to 0.5% w/v PVA solution (100 mL) containing tween 20 (1% w/v) to develop double emulsion. Subsequently, emulsion was continuously stirred at 1500 rpm for 3 h on magnetic stirrer (REMI, Mumbai, India) at 37 ± 0.5 °C. Hardened microspheres were filtered through 0.45 µm millipore filter, and washed thrice with petroleum ether succeeded by ultracentrifugation using cooling centrifuge (Remi, RIS-24 BL, Mumbai, India) at 10,000 rpm for 15 min at 4 °C. Freeze-drying was performed at −65 °C and 0.5 kPa vacuum in lyophilizer (Allied Frost, India) using D-mannitol as lyoprotectant to acquire fine powder.

Figure 2. Formulation strategy of NPH-MS.

Display full size

Determination of entrapment efficiency (% EE), mean diameter and yield

Entrapment efficiency was determined by analyzing amount of unentrapped drug in supernatant recovered after centrifugation (Remi, RIS-24 BL, Mumbai, India) of NPH-MS at 5000 rpm for 10 min. Analysis was performed by double beam UV–visible spectrophotometer (Systronics AU-2701, Ahmedabad, India) at 266 nm [13,14]. The following formula was used to determine % EE.

(1)

Mean diameters of NPH-MS were determined using APCAM USB2 digital cameras system (APCAM, India). Measurement was executed in triplicate ($n = 3$) to obtain mean diameter [14].

Percent yield was calculated as weight percentage of completely dried microspheres recovered from each experimental, with respect to initial total weight of NPH, PHB and PCL using following equation:

(2)

Fourier transform infrared spectroscopy (FTIR)

Spectra of NPH, PHB, PCL, physical mixture and NPH-MS were

recorded using IR Affinity-1, Shimadzu (Germany) spectrometer to confirm drug–polymer compatibility and entrapment of NPH in polymeric matrix. FTIR spectra of samples were scanned in analytical range of 400–4000 cm^{-1} using KBr disks at ambient temperature.

Powder X-ray diffraction studies (PXRD)

X-ray diffraction patterns of samples were obtained on Xpert-Pro diffractometer in continuous scan mode over an angular range $2\theta = 5°$ to $2\theta = 50°$ using 1.54 A° CuKα radiation and 1.39 A° CuKβ radiation generated by tube operated at 45 kV, 40 mA.

Laser diffractometry analysis

Mean diameter and size distributions of microspheres were determined by laser diffractometry using mastersizer 2000 ver. 5.61 (Malvern Instruments Ltd., Malvern, UK). The sample was dispersed in water having refractive index 1.330. Analysis was carried out in triplicate. Particle size distributions (span) were calculated using the following equation [14]:

(3)

where, $d(0.1)$, $d(0.5)$ and $d(0.9)$ are particle diameter at 10, 50 and 90% of undersized particle distribution curve.

Zeta potential (ζ) analysis and scanning electron microscopy (SEM)

Zeta potential of NPH-MS was measured by establishing electrophoretic mobility employing zetasizer *ver.* 7.03 (Malvern Instruments Ltd., Malvern, UK) in disposable zeta cell at count rate of 29.3 kcps at 25 °C. Scanning electron micrograph of NPH-MS was recorded using Hitachi S3400N (Japan) scanning electron microscope to assess surface morphology. Freeze dried microspheres were mounted onto aluminium stub using double-sided adhesive tape and then sputter coated with a thin layer of gold to attain 20 nm film using Coater Polaron at 1.4 kV.

In-vitro drug release study

In-vitro drug release profiles from NPH, physical mixture and NPH-MS were studied in phosphate buffer (pH 7.4) using pre-treated dialysis membrane (Himedia, India) having molecular weight cut-off (MWCO) of ~12,000–14,000 Da [15]. Dialysis bag containing NPH-MS (equivalent to 180 mg NPH) was dipped in 100 mL of phosphate buffer (pH 7.4), and flask was placed in

shaking incubator maintained at 100 rpm and 37 ± 0.5 °C [12,16,17]. Samples were withdrawn periodically and reloaded with equivalent volume of dissolution medium. Quantitation was performed at 266 nm using double beam UV–visible spectrophotometer. For comparison of drug release profile, mean dissolution time (MDT) of NPH, physical mixture, NPH-MS was determined using the following equation:

(4)

where, n is number of dissolution times; j is sample number; $\hat{t}_j$ is the time at mid-point and ΔM_j is additional amount of drug dissolved between t_j and t_{j-1} [18].

Haemocompatibility study

Haemolytic toxicity analysis was executed according to ISO 10993-4 standards. Whole blood was collected from healthy volunteer in citrated tubes (3.8% sodium citrate) to restrain spontaneous coagulation. The erythrocytes were separated by centrifugation at 2500 rpm (REMI, Mumbai, India) for 10 min at room temperature and re-suspended in normal saline solution. The centrifugation and discarding of supernatant were repeated thrice followed by re-suspending the RBCs in 10 mL phosphate-buffered saline (pH 7.4). 50 µL solution of NPH, blank and drug-loaded microspheres was added to 1 mL of RBC suspension and incubated at 37 °C for 90 min in an incubator (Remi, India). Subsequently, samples were centrifuged at 2500 rpm for 5 min, and absorbance of supernatant was measured at 545 nm using UV–visible spectrophotometer (Systronics AU-2701, Ahmedabad, India). Phosphate buffer saline (PBS) with 0% haemolysis was taken as the negative control and the positive control comprised of double-distilled deionized water with 100% haemolysis [19]. The experiment was performed in triplicate. The percent haemolysis was calculated using the following equation:

(5)

Antinociceptive activity by tail-flick latency test

The animal experiments have been performed by following experimental protocol guidelines of committee for purpose of control and supervision of experiments on animals (CPCSEA) governed under ministry of environment and forest, government of India. Animal experiments were conducted after ethical clearance by institutional animal ethics committee (IAEC/CCP/14/PR-017 and IAEC/CCP/16/PR-013). Wistar rats (180–

200 g) were indiscriminately divided into five experimental groups (*n* = 5 rats/group). Phosphate buffer saline (5 mL/kg) and NPH (20 mg/kg) were administered *via* peroral route to control and reference group, respectively. Test groups were administered NPH-MS ~10, 20 and 30 mg/kg NPH to estimate ED_{50}. Tails of animals were located on radiant heat source of digital analgesiometer (Inco Instruments & Chemical Pvt. Ltd., Ambala, India). A cut-off period of 12 s was permitted to restrain tissue injury. End point was tail withdrawal with sharp flicking response. Minimum 3–5 basal reaction times at gap of 5 min were recorded prior to administration of medicine to validate normal behaviour of animals. Rats indicating baseline latency time >3 s were repudiated from investigation [20,21]. Post-dose latency time was recorded at definite time intervals *i.e.* 1, 2, 4, 8, 12 and 24 h and transformed to percentage maximum possible effect (% MPE) using following equation:

(6)

Dose-related antinociceptive effects of NPH-MS were plotted for % MPE *vs.* log dose. Effective dose that produced 50% of the maximum possible effect (ED_{50}) was calculated using four-parameter logistic equation with the top or bottom fixed through curve-fitting functions in GraphPad Prism version 5.01 (San Diego, CA) [22].

Post-operative pain model

Surgical procedure

Incisional pain was induced in rats as described by Brennan et al. [23,24]. Using 10 # scalpel, longitudinal incision of 1 cm was made on plantar surface of left hind paw of rats after anaesthetization with 2% isofluorane. The incision was started from 0.5 cm proximal periphery of heel and extended to toes. The plantaris muscle was elevated using forceps and closed longitudinally with two mattress sutures using 5-0 nylon with gentle pressure. The wound site was sprinkled with povidine–iodine solution (Cipladine, Cipla Ltd. Mumbai, India) and rats recovered from the anaesthesia in their home cages [25,26].

Treatment of injury

Wistar rats were divided into four groups (*n* = 5 rats/group). PBS-treated (control), NPH-treated (reference), NPH-MS-treated (test) and sham group. Sham-operated animals received anesthesia,

but not an incision. Effective dose (ED_{50}) of NPH-MS estimated through tail flick study was administered to test group incisioned rats. For treatment of injury, drugs were administered 30 min prior to surgery on day 0, and continued daily to day 14 post-ligation. To fulfill the ethical requirements, behavioral tests were performed on randomly selected day. Experiments were performed before surgery on day 0 (baseline-BL), and day 5 post-surgery, at time periods (1, 2, 4, 8, 12, 24 h) post-dose. The magnitude of reversal of mechanical allodynia and thermal hyperalgesia in rats of different groups was investigated. The person performing behavioural tests was blinded to the drug administration.

Von frey's test

VFWT to noxious mechanical stimulus was determined using an automated electronic von frey (IITC Life Sciences, Woodland Hills, CA). Rats were located in individual Plexiglas chambers on top of a metal screen surface having 1 cm mesh openings, elevated 50 cm above the laboratory bench top and acclimatized to the environment for 30 min prior to test. An increasing force in grams (mechanical allodynia) was applied to plantar surface of left hind incisioned paw of individual animal using non-flexible filament of von frey apparatus and nocifensive paw withdrawal (VFWT) was considered as end point. Average VFWTs were determined from three thresholds per test [26,27].

Plantar test

PWL to noxious heat stimulus was assessed to evaluate the magnitude of thermal hyperalgesia. Rats were located on a clean glass surface covered with clear plastic cage and focused radiant heat source (EKE, Tokyo, Japan) was applied beneath the glass floor at middle of plantar incision to determine PWLs. Radiant beam intensity was adjusted such that the baseline PWL at day 0 for all animals of each group prior to surgery was 9 ± 0.5 s. A maximal cut-off value was taken 20 s to preclude tissue damage. PWLs were determined from the average of three experiments performed at 10-min interval to avoid thermal sensitization [24,28,29].

Statistical analysis

All the experiments were performed in triplicate, and results were expressed as mean ± SEM ($n = 3$). Statistical analysis was

performed using using GraphPad Prism version 5.01 (San Diego, CA). Data were analyzed by analysis of variance (ANOVA) followed by Bonferroni *post hoc* test. $p \leq 0.05$ was considered statistically significant as compared with control and reference group.

Results and discussion

Fourier transform infrared spectroscopy

FTIR spectra of NPH (Figure 3(a)) demonstrated characteristic peaks of C–O–C of cyclic ring (3429 cm^{-1}), C–H stretch of alkane (2910 cm^{-1}, 2428 cm^{-1}), C = C of aromatics (1446 cm^{-1}), C–N of amines (1346 cm^{-1}), C–O stretch (1024 cm^{-1}) and aromatic ring (759 cm^{-1}). FTIR spectra of PCL (Figure 3(b)) showed significant peaks of O–H (s) of carboxylic acid (3439 cm^{-1}), C–H stretch of alkane (2947 cm^{-1}), C = O of carboxylic acid (1732 cm^{-1}), C–H (b) of alkane (1471 cm^{-1}), C–O–H bond (1365 cm^{-1}) and C–O (s) of COOH (1178 cm^{-1}) (18,22). FTIR spectra of PHB (Figure 3(c)) illustrated distinctive peaks of O–H (s) of carboxylic acid (3439 cm^{-1}), C–H (s) of alkane (2978 cm^{-1}), C = O (s) of carboxylic acid (1728 cm^{-1}), C–H (b) of alkane (1454 cm^{-1}), C–O–H bond (1286 cm^{-1}, 1381 cm^{-1}) and C–O (s) of COOH (1055 cm^{-1}, 1184 cm^{-1}). Characteristic absorption peaks of NPH, PHB and PCL remained integral in physical mixture which revealed compatibility between drug and polymers (Figure 3(d)). FTIR spectra of NPH-MS illustrated prominent absorption peaks of NPH, PHB and PCL that implied absence of significant molecular interaction between drug and polymers and confirmed that NPH was successfully incorporated into matrix (Figure 3(e)) [13,14,30].

Figure 3. FTIR spectra of (a) NPH, (b) PCL, (c) PHB, (d) physical mixture, and (e) NPH-MS.

Display full size

X-ray diffraction studies

X-ray diffractogram of NPH displayed characteristic crystalline peaks at 2θ scattered angles of 7.7°, 12.36°, 13.9°, 15.75°, 16.89°, 18.12°, 19.76°, 23.03°, 26.27°, 35.23° and 40.53° which showed abundantly crystalline characteristics of drug (Figure 4(a)). X-ray diffractogram of PCL exemplified crystalline peaks at 21.54°,

22.15° and 23.81° (Figure 4(b)). X-ray diffractogram of PHB illustrated crystalline peaks at 13.53°, 16.93°, 20.15°, 21.62°, 22.59°, 25.54° and 27.13° (Figure 4(c)). X-ray diffractograms of physical mixture demonstrated existence of crystalline peaks of NPH, PHB and PCL that implied absence of incompatibility between drug and polymers (Figure 4(d)). The distinguishing crystalline peaks of NPH were not perceived in NPH-MS which accredited that drug was entrapped in amorphous form in polymer matrix (Figure 4(e)) [13,14].

Figure 4. X-ray diffraction patterns of (a) NPH, (b) PCL, (c) PHB, (d) physical mixture, and (e) NPH-MS.

Display full size

Laser diffractometry analysis

Surface weighted mean diameter of microspheres using laser diffractometry was found 189.4 µm. The value of *d*(0.1), *d*(0.5) and *d*(0.9) was 133.664, 335.191 and 758.461 µm, respectively. Calculated span value for NPH-MS was found 1.864 (< 2), which revealed uniform particle size distribution [14].

Zeta potential (ζ) and scanning electron microscopy analysis

Zeta potential value of NPH-MS was found −17 mV which might be caused by deposition of PVA on surface of microspheres with its hydrophobic tail embedded into PHB (having hydrophobic nature) while hydrophilic polar end projected outside. Scanning electron microscopic image displayed that microspheres were spherical shaped with smooth surface morphology (Figure 5).

Figure 5. Scanning electron microscopic image of NPH-MS.

Display full size

In-vitro drug release study

NPH and physical mixture delivered % cumulative drug release (CDR) of 83.52% and 79.86% within 2 h, respectively, whereas NPH-MS revealed biphasic release pattern with an initial burst effect equivalent to about 35.51% in 2 h, succeeded by slow sustained effect corresponding to 68.32% in 12 h and 79.75% in

24 h (Figure 6). The preliminary rapid release of drug could be illustrated by drug desorption from larger external specific surface of microspheres [17,31]. MDT for NPH, physical mixture and NPH-MS was found 1.52, 1.84 and 6.73 h, respectively, which revealed gradual drug release behaviour from NPH-MS in comparison to NPH.

Figure 6. *In-vitro* drug release profile of NPH-MS in comparison to NPH and physical mixture in PBS.

Display full size

Haemocompatibility study

Haemolysis analysis gives quantitative estimation about iron-containing protein haemoglobin release due to potential damage to RBC's. Percentage haemolysis of NPH, blank and drug-loaded microspheres (NPH-MS) were found 13.33 ± 0.23, 2.5 ± 0.2 and 2.8 ± 0.24, respectively (Figure 7). It was observed that NPH cause significant haemolysis as compared with blank and drug loaded-microspheres ($p < .05$). Since, NPH-MS has negative surface charge, consequently displayed less haemolytic activity with negatively charged RBCs. It was apparent from this investigation that PHB/PCL microspheres significantly suppressed the haemolytic toxicity of NPH. Haemocompatibility tests of drug-loaded microspheres indicated that the haemolysis was <5% which signified that formulation was highly haemocompatible, demonstrating its biocompatibility.

Figure 7. Percentage haemolysis of red blood cells by NPH, blank microspheres and NPH-MS.

Display full size

Antinociceptive activity by tail-flick latency test

Tail-flick latency time (s) observed for NPH-MS (10–30 mg/kg) was statistically insignificant as compared with NPH 20 mg/kg for preliminary 2 h post-dose ($p > .05$), followed by statistically significant difference till 24 h ($p < .001$) (Figure 8). This illustrated that NPH-MS exhibited sustained antinociceptive effect in comparison to NPH. Furthermore, it was observed that 30 mg/kg of microspheres exhibited maximum anti-nociceptive effect, %

MPE (91.68 ± 7.63%) followed by 20 mg/kg (81.61 ± 4.45%) and 10 mg/kg (61.66 ± 6.85%) which indicates dose-dependent antinociceptive effect in rat model (Figure 9). Once-daily dose, producing 50% maximum possible effect (ED_{50}) in rat model estimated through curve-fitting functions of GraphPad Prism 5.01 was found NPH-MS ~18.12 mg/kg NPH.

Figure 8. Tail withdrawal latency time from various doses of NPH-MS administered via peroral route ($n = 5$ rats per group). *$p < .05$, ***$p < .001$ compared with NPH treated rats.

Display full size

Figure 9. Anti-nociceptive effects of NPH-MS (p.o) in tail flick test (a) time-related effects, and (b) dose-related effects. **$p < .01$, ***$p < .001$ compared with NPH treated rats.

Display full size

Incisional pain model

Time course of mechanical allodynia in incisioned rats was measured by von Frey test. Control group showed significant reduction in VFWT at all-time points (17.23 ± 2.18 g to 32.1 ± 3.15 g) as compared with baseline (72.4 ± 3.2 g), whereas the withdrawal threshold in sham-operated rats was 70.4 ± 1.2 g. NPH (20 mg/kg) significantly attenuated ($p < .001$) mechanical allodynia for initial 4 h post-dose ($p < .01$, $p < .001$), followed by insignificant inhibition of allodynia till 24 h ($p > .05$), as compared to control group. In contrast, NPH-MS significantly reversed the allodynia till 24 h ($p < .001$). Bonferroni *post hoc* test illustrated that VFWT for NPH-MS (56.23 ± 2.1 g) was statistically insignificant as compared to pure drug (47.10 ± 2.4 g) for preliminary 2 h post-dose ($p > .05$), followed by statistically significant difference till 24 h ($p < .001$) (Figure 10).

Figure 10. Effect of NPH-MS (p.o) on the paw withdrawal threshold as tested by von Frey test ($n = 5$ rats per group). *$p < .05$, ***$p < .001$ compared with NPH treated rats, ‡$p < .001$ compared with the control group.

Display full size

To determine whether NPH-MS affect thermal hyperalgesia, the plantar test was performed. Control group illustrated significant reduction in PWL at all-time points (3.1 ± 0.7 s to 3.7 ± 0.6 s) as compared with baseline (8.7 ± 0.2 s), while latency in sham-operated rats was 8.65 ± 0.25 s. Bonferroni *post hoc* test signified that PWL for NPH-MS (6.7 ± 0.61 s) was statistically insignificant in comparison to NPH 20 mg/kg (6.6 ± 0.46 s) for initial 2 h post-dose ($p > .05$), succeeded by substantial difference till 24 h ($p < .001$). Incisional pain study revealed that sustained release NPH-MS possibly will be beneficial therapeutic aspect for management of post-operative pain (Figure 11).

Figure 11. Effect of NPH-MS (p.o) on the PWL as tested by plantar test ($n = 5$ rats per group). *$p < .05$, **$p < .01$ compared with NPH treated rats, †$p < .01$, ‡$p < .001$ compared with the control group.

Display full size

Conclusions

In current investigation, nefopam hydrochloride-loaded poly-(ε-caprolactone) and poly-3-hydroxybutyrate biodegradable microspheres were successfully developed by double emulsion solvent evaporation technique. *In-vitro* drug release study of NPH-MS revealed biphasic pattern with an initial burst succeeded by sustained drug release behavior till 24 h. Percentage haemolysis of NPH-MS was found 2.8 ± 0.24 which revealed its haemocompatibility. ED_{50} of drug-loaded microspheres estimated through tail-flick anti-nociceptive test in rat model was found ~18.12 mg/kg NPH. This dose could significantly alleviate mechanical allodynia and thermal hyperalgesia till 24 h, as compared with NPH 20 mg/kg which merely produced effect till 2–4 h. It was concluded that once-daily oral dose of NPH-MS could appreciably be utilized for management of acute post-surgical pain which might augment patient-compliance furthermore.

Acknowledgements

The authors are thankful to IKG Punjab Technical University, Jalandhar, for providing access to ScienceDirect and turnitin

software. The authors express gratitude to Chitkara University for infrastructural support to carry out this work.

Disclosure statement

The authors declare that they have no competing interests.

References

1. De Jong WH, Borm PJA. Drug delivery and nanoparticles: applications and hazards. Int J Nanomedicine. 2008;3:133–149. [Crossref], [PubMed], [Web of Science ®], [Google Scholar]

2. Aymard G, Warot D, Demolis P, et al. Comparative pharmacokinetics and pharmacodynamics of intravenous and oral nefopam in healthy volunteers. Pharmacol Toxicol. 2003;92:279–286. [Crossref], [PubMed], [Google Scholar]

3. Kyung HK, Salahadin A. Rediscovery of nefopam for the treatment of neuropathic pain. Korean J Pain. 2014;27:103–111. [Crossref], [PubMed], [Google Scholar]

4. Hamishehkar H, Emami J, Najafabadi AR, et al. The effect of formulation variables on the characteristics of insulin-loaded poly(lactic-co-glycolic acid) microspheres prepared by a single phase oil in oil solvent evaporation method. Colloids Surf B Biointerfaces. 2009;74:340–349. [Crossref], [PubMed], [Web of Science ®], [Google Scholar]

5. Abraham GA, Gallardo A, San Roman J, et al. Polymeric matrices based on graft copolymers of PCL onto acrylic backbones for releasing antitumoral drugs. J Biomed Mater Res. 2003;64:638–647. [Crossref], [Web of Science ®], [Google Scholar]

6. Chun YS, Kim WN. Thermal properties of poly (hydroxybutyrate-co-hydroxyvalerate) and poly (ε-caprolactone) blends. Polymer. 2000;41:2305–2308. [Crossref], [Web of Science ®], [Google Scholar]

7. Marin E, Briceño MI, Caballero-George C. Critical evaluation of biodegradable polymers used in nanodrugs. Int J Nanomedicine. 2013;8:3071–3090. [PubMed], [Web of Science ®], [Google Scholar]

8. El-Hadi A, Schnabel R, Straube E, et al. Correlation between degree of crystallinity, morphology, glass temperature, mechanical properties and biodegradation of poly (3-hydroxyalkanoate) PHAs and their blends. Polymer Testing. 2002;21:665–674. [Crossref], [Web of Science ®], [Google Scholar]

9. Sinha VR, Bansal K, Kaushik R, et al. Poly-epsilon-caprolactone microspheres and nanospheres: an overview. Int J Pharm. 2004;278:1–23. [Crossref], [PubMed], [Web of Science ®], [Google Scholar]

10. Youan BB, Benoit MA, Baras B, et al. Protein-loaded poly(epsilon-caprolactone) microparticles. I. Optimization of the preparation by (water-in-oil)-in water emulsion solvent evaporation. J Microencapsul. 1999;16:587–599. [Taylor & Francis Online], [Web of Science ®], [Google Scholar]

11. Francis L, Meng D, Knowles J, et al. Controlled delivery of gentamicin using poly(3-hydroxybutyrate) microspheres. Int J Mol Sci. 2011;12:4294–4314. [Crossref], [PubMed], [Web of Science ®], [Google Scholar]

12. Raval JP, Naik DR, Amin KA, et al. Controlled-release and antibacterial studies of doxycycline-loaded poly (ε-caprolactone) microspheres. J Saudi Chem Soc. 2014;18:566–573. [Crossref], [Web of Science ®], [Google Scholar]

13. Gajra B, Dalwadi C, Patel R. Formulation and optimization of itraconazole polymeric lipid hybrid nanoparticles (Lipomer) using box behnken design. Daru J Pharm Sci. 2015;23:3–18. [Crossref], [Web of Science ®], [Google Scholar]

14. Natarajan V, Krithica N, Madhan B, et al. Formulation and evaluation of quercetin polycaprolactone microspheres for the treatment of rheumatoid arthritis. J Pharm Sci.

2011;100:195–205. [Crossref], [PubMed], [Web of Science ®], [Google Scholar]

15. D'Souza S. A review of *in-vitro* drug release test methods for nano-sized dosage forms. Adv Pharm. 2014;2014:1–12. [Google Scholar]

16. Kumar A, Sawant K. Encapsulation of exemestane in polycaprolactone nanoparticles: optimization, characterization, and release kinetics. Cancer Nanotechnol. 2013;4:57–71. [Crossref], [PubMed], [Google Scholar]

17. Singh S, Muthu MS. Studies on biodegradable polymeric nanoparticles of risperidone: in vitro and in vivo evaluation. Nanomedicine (Lond). 2007;3:305–319. [Web of Science ®], [Google Scholar]

18. Costa P, Sousa Lobo JM. Modeling and comparison of dissolution profiles. Eur J Pharm Sci. 2001;13:123–133. [Crossref], [PubMed], [Web of Science ®], [Google Scholar]

19. Khatik R, Dwivedi P, Shukla A, et al. Development, characterization and toxicological evaluations of phospholipids complexes of curcumin for effective drug delivery in cancer chemotherapy. Drug Deliv. 2016;23:1057–1068. [Taylor & Francis Online], [Web of Science ®], [Google Scholar]

20. Brady LS, Holtzman SG. Analgesic effects of intraventricular morphine and enkephalins in nondependent and morphine-dependent rats. J Pharmacol Exp Ther. 1982;222:190–197. [PubMed], [Web of Science ®], [Google Scholar]

21. D'Amour FE, Smith DL. A method for determining loss of pain sensation. J Pharmacol Exp Ther. 1941;72:74–79. [Google Scholar]

22. Jones CK, Peters SC, Shannon HE. Efficacy of duloxetine, a potent and balanced serotonergic and noradrenergic reuptake inhibitor, in inflammatory and acute pain models in rodents. J Pharmacol Exp Ther. 2005;312:726–732. [Crossref], [PubMed], [Web of Science ®], [Google Scholar]

23. Brennan TJ, Vandermeulen EP, Gebhart GF. Characterization of a rat model of incisional pain. Pain. 1996;64:493–501. [Crossref], [PubMed], [Web of Science ®], [Google Scholar]

24. Hamalainen MM, Subieta A, Arpey C, et al. Differential effect of capsaicin treatment on pain-related behaviors after plantar incision. J Pain. 2009;10:637–645. [Crossref], [PubMed], [Web of Science ®], [Google Scholar]

25. Suto T, Obata H, Tobe M, et al. Long-term effect of epidural injection with sustained-release lidocaine particles in a rat model of postoperative pain. Br J Anaesth. 2012;109:957–967. [Crossref], [PubMed], [Web of Science ®], [Google Scholar]

26. Whiteside GT, Harrison J, Boulet J, et al. Pharmacological characterisation of a rat model of incisional pain. Br J Pharmacol. 2004;141:85–91. [Crossref], [PubMed], [Web of Science ®], [Google Scholar]

27. Stuesse SL, Crisp T, McBurney DL, et al. Neuropathic pain in aged rats: behavioral responses and astrocytic activation. Exp Brain Res. 2001;137:219–227. [Crossref], [PubMed], [Web of Science ®], [Google Scholar]

28. Hargreaves K, Dubner R, Brown F, et al. A new and sensitive method for measuring thermal nociception in cutaneous hyperalgesia. Pain. 1988;32:77–88. [Crossref], [PubMed], [Web of Science ®], [Google Scholar]

29. Zahn PK, Brennan TJ. Primary and secondary hyperalgesia in a rat model for human postoperative pain. Anesthesiology. 1999;90:863–872. [Crossref], [PubMed], [Web of Science ®], [Google Scholar]

30. Zhou YZ, Alany RG, Chuang V, et al. Optimization of PLGA nanoparticles formulation containing L-DOPA by applying the central composite design. Drug Dev Ind Pharm. 2013;39:321–330. [Taylor & Francis Online], [Web of Science ®] , [Google Scholar]

31. Karasulu E, Yeşim Karasulu H, Ertan G, et al. Extended release lipophilic indomethacin microspheres: formulation factors and

mathematical equations fitted drug release rates. Eur J Pharm Sci. 2003;19:99–104. [Crossref], [PubMed], [Web of Science ®], [Google Scholar]

Browse journals by subject

Back to top

Area Studies

Arts

Behavioral Sciences

Bioscience

Built Environment

Communication Studies

Computer Science

Development Studies

Earth Sciences

Economics, Finance, Business & Industry

Education

Engineering & Technology

Environment & Agriculture

Environment and Sustainability

Food Science & Technology

Geography

Health and Social Care

Humanities

Information Science

Language & Literature

Law

Mathematics & Statistics

Medicine, Dentistry, Nursing & Allied Health

Museum and Heritage Studies

Physical Sciences

Politics & International Relations

Social Sciences

Sports and Leisure

Tourism, Hospitality and Events